Global simulations of carbon allocation coefficients for deciduous vegetation types

By JIANGZHOU XIA[1], YANG CHEN[1], SHUNLIN LIANG[2,3], DAN LIU[1] and WENPING YUAN[1]*, *[1]State Key Laboratory of Earth Surface Processes and Resource Ecology, Beijing Normal University, Beijing 100875, China; [2]State Key Laboratory of Remote Sensing Science, School of Geography, Beijing Normal University, Beijing 100875, China; [3]Department of Geographical Sciences, University of Maryland, College Park, MD 20742, USA*

ABSTRACT

The allocation of photosynthate among the plant components plays an important role in regulating plant growth, competition and other ecosystem functions. Several process-based carbon allocation models have been developed and incorporated into ecosystem models; however, these models have used arbitrary model parameters and have never been sufficiently validated on a global scale. This study uses the Integrated Biosphere Simulator (IBIS) model as a platform to integrate a carbon allocation model (resource availability model) with satellite-derived leaf area index (LAI) dataset, which allows us to inversely predict the allocation parameters for five deciduous vegetation types. Our results showed that the carbon allocation coefficients can be reliably constrained by the satellite LAI product, and the new parameters substantially improved model performance for simulating LAI and aboveground biomass globally. The spatial pattern of allocation coefficients among plant parts is supported by a number of studies. Compared with the standard version of the IBIS model using fixed allocation coefficients, the revised resource availability carbon allocation model tends to promote higher root carbon allocation. Our study provides a method for inverting the parameters of the carbon allocation model and improves the model performance in simulating the LAI and biomass.

Keywords: carbon allocation, resource availability, leaf area index, Bayesian inversion, Integrated Biosphere Simulator

1. Introduction

Carbon allocation refers to the allocation of photosynthate among plant parts (e.g. leaves, stems and roots), which profoundly impacts plant growth, competition and the terrestrial ecosystem carbon cycle (Friedlingstein et al., 1999; Bonan, 2008; Malhi et al., 2011; McMurtrie and Dewar, 2013). Climate change has substantially changed carbon allocation processes as well as leaf area index (LAI), vegetation height and rooting depth, which impact land surface albedo; roughness; radiative exchange; and carbon, water and energy fluxes (Gorissen et al., 2004; De Kauwe et al., 2014). Those changes result in the profound feedbacks to the climate system from terrestrial ecosystems (Bonan, 2008). Therefore, reliable estimations of carbon allocation are crucial for understanding the terrestrial carbon cycle and predicting future climate change.

Several methods have been used to estimate carbon allocation among plant components within ecosystem models. Some models, such as CASA (Potter et al., 1993), Integrated Biosphere Simulator (IBIS) (Foley et al., 1996; Kucharik et al., 2000) and Hyland (Levy et al., 2004), apply the simplest approach to simulate carbon allocation processes by assuming temporally and spatially constant allocation coefficients among roots, stems and leaves. Obviously, this method is too simplistic to accurately reproduce principal processes and dynamics of carbon allocation (Gower et al., 1999). Some process-based carbon allocation models have been developed by incorporating physiological and biochemical mechanisms. Several models estimate carbon allocation based on allometric constraints (e.g. leaf mass/woody mass or leaf mass/root mass ratios), such as FBM (Kindermann et al., 1993), BIOME-3 (Haxeltine and Prentice, 1996), Hybrid (Friend et al., 1997) and ED (Moorcroft et al., 2001). The LPJ model (Sitch et al., 2003) uses a pipe model to estimate leaf biomass, which states that there is fixed proportionality between the leaf area and the sapwood

*Corresponding author.
email: yuanwpcn@126.com

1

cross-sectional area (equivalent to the quantity of transport tissue) (Shinozaki et al., 1964a, 1964b). In addition to the pipe model, the relative allocation to roots versus leaves and sapwood in the LPJ model depends on experienced water deficit. However, these carbon allocation models do not or seldom integrate the regulations of comprehensive environment factors in carbon allocation simulations, such as light and nutrients availabilities (Franklin et al., 2012; Doughty et al., 2013).

There has been a long history of determining the growth ratio response of plant components (e.g. roots, shoots) to changes in water, nutrients and light availability (Wilson, 1988; Cannell and Dewar, 1994; Bazzaz and Grace, 1997). Therefore, a growing body of studies highlights environmental parameters, including resource availability (i.e. water, nutrient and light), that greatly influence carbon allocation (Tilman, 1988). A plant in an optimal environment achieves maximum growth by allocating all new photosynthesis products to leaves (Monsi and Saeki, 1953; Chapin, 1991). In nature, however, environmental stresses compromise this allocation pattern and compel plants to invest in stems for light capturing and roots for obtaining water and nutrients (Friedlingstein et al., 1999). Based on the principle of environmental resource availability, Friedlingstein et al. (1999) developed a global allocation scheme that estimates the allocation of photosynthate among leaves, stems and roots depending on availability of water, light and mineral nitrogen. The philosophy of the resource availability model (RACA) is that carbon allocation results from the response that regulates carbon investments to help capture the most limiting resources (i.e. water, light or nutrients). Compared with the previous method, this method has a strong theoretical basis and has been used in numerous ecosystem models, including CTEM (Arora and Boer, 2005), ORCHIDEE (Krinner et al., 2005) and aDGVM (Scheiter and Higgins, 2009). However, the carbon allocation parameters to plant parts for non-limiting conditions are not well constrained. Furthermore, it is difficult to validate the carbon allocation model on a large scale (Friedlingstein et al., 1999).

In this study, IBIS model was modified to incorporate dynamic allocation based on RACA. We used satellite-based LAI to inversely predict the carbon allocation parameters and validate a resource availability model because LAI is tightly related to carbon allocation in terrestrial ecosystem models and provides unprecedented spatial coverage and resolution for validating the carbon allocation model on a large scale. The primary objectives of this study are to (1) inversely predict the parameters of resource availability allocation model, (2) assess the performance of the modified version of IBIS and (3) analyse the variation characteristics of carbon allocation coefficients changing along with resource availabilities.

2. Materials and methods

2.1. Resource availability carbon allocation method

Sharpe and Rykiel (1991) initially developed a relationship for describing the regulation of resource availability to a given plant part:

$$A \propto \frac{\sum X_i}{\sum X_i + \sum Y_j} \qquad (1)$$

where A is the allocation of photosynthate to a given part (i.e. leaves, stems and roots). X_i and Y_j are the availabilities of two resources (e.g. light, water and nutrients) that lead to increase or decrease in carbon allocation to that part, respectively. For example, for plant roots, water availability is a Y-type resource, and root allocation will decrease if water is sufficient because it is not needed to promote root growth to enhance water uptake.

In this study, we used the allocation equations proposed by Friedlingstein et al. (1999). The allocation coefficients of leaves (*aleaf*), stems (*astem*) and roots (*aroot*) are expressed as

$$aroot = 3r_0 \frac{L}{L + 2\min(W, N)} \qquad (2)$$

$$astem = 3s_0 \frac{\min(W, N)}{2L + \min(W, N)} \qquad (3)$$

$$aleaf = 1 - astem - aroot \qquad (4)$$

where $\min(W, N)$ is the minimum availability of water (W) and nitrogen (N), and r_0 and s_0 are the allocation fractions of roots and stems under the non-limiting condition, respectively. The two carbon allocation parameters (i.e. r_0 and s_0) were inversely predicted using the Monte Carlo Markov Chain (MCMC) method in this study.

We used the original equation to calculate the nitrogen constraint equation and revised the equations for water and light constraints. For each month, we used the cloud fraction to estimate the light availability (L) as

$$L = 1 - cld \qquad (5)$$

where *cld* is the monthly total cloud fraction.

The ratio of evapotranspiration (ET) to potential evapotranspiration (PET) is used to indicate water availability (Mu et al., 2013). The monthly water availability (W) is calculated by

$$W = \frac{ET}{PET} \qquad (6)$$

The ET was calculated using a revised remote-sensing Penman Monteith (Revised RS-PM) model (Yuan et al., 2010; Chen et al., 2014). The PET was calculated according to the Penman Monteith model (Monteith, 1965).

Nitrogen availability (N) is calculated by combining the temperature (T_s) and moisture (W_s) limitations (Friedlingstein et al., 1999). The temperature limitation was calculated based on a standard Q_{10} equation (Potter et al., 1993), and the moisture limitation was modelled following the method of Parton et al. (2001).

$$N = T_s \times W_s \qquad (7)$$

$$T_s = Q_{10}^{\left(\frac{T-30}{10}\right)} \qquad (8)$$

$$W_s = \frac{1}{1 + 30 \times e^{-8.5(PPT/PET)}} \qquad (9)$$

where T is the monthly mean air temperature (°C), PPT is the monthly precipitation (mm) and $Q_{10} = 2$.

2.2. LAI simulation

To retrieve accurate carbon allocation parameters, we eliminated the impacts of the uncertainties of phenology and LAI simulations using the satellite data. Moderate Resolution Imaging Spectroradiometer (MODIS) Land Cover Dynamics (MCD12Q2) product (i.e. Global Vegetation Phenology product) was used to identify the start (T_o) and end dates (T_e) of the growing season of the five deciduous vegetation types from 2000 to 2010 (Fig. 1). Moreover, based on the global satellite-based LAI data, the dates and magnitude of maximum LAI (T_m) were determined. For simulating LAI that was calculated using the RACA model (LAI$_{RACA}$), a linear increase from 0 to 25% of maximum

LAI was assumed to occur within the first 15 d of the growing season. After that, the specific leaf area method was used to simulate LAI increases until to T_m [eq. (10)]. From T_m to T_e, new photosynthate would not allocate to leaf part, and LAI decreased from simulated maximum LAI to zero following the curves of leaf falling retrieved from satellite LAI data. In comparison with LAI$_{RACA}$, following the same method, we also simulated LAI (LAI$_{IBIS}$) using IBIS with the constant carbon allocation coefficients (Table 1).

$$LAI = NPP \times aleaf \times SLA \qquad (10)$$

where NPP is the net primary productivity; a satellite-based light-use efficiency model (i.e. EC-LUE, Yuan et al., 2007, 2010) was used to calculate gross primary production (GPP), and then NPP was calculated as half of GPP (Fung et al., 2005; Waring and Running, 2010); *aleaf* is the carbon allocation coefficient of leaves; SLA is the specific LAI (25 m^2 kg C^{-1}, Foley et al., 1996).

2.3. Datasets

Regional NPP and resource availabilities were estimated based on the satellite observed monthly vegetation attributes and monthly surface meteorology inputs. The biweekly GIMMS NDVI with 8-km spatial resolution from 2000 to 2006 has been corrected for calibration, view geometry, volcanic aerosols and other effects not related to vegetation
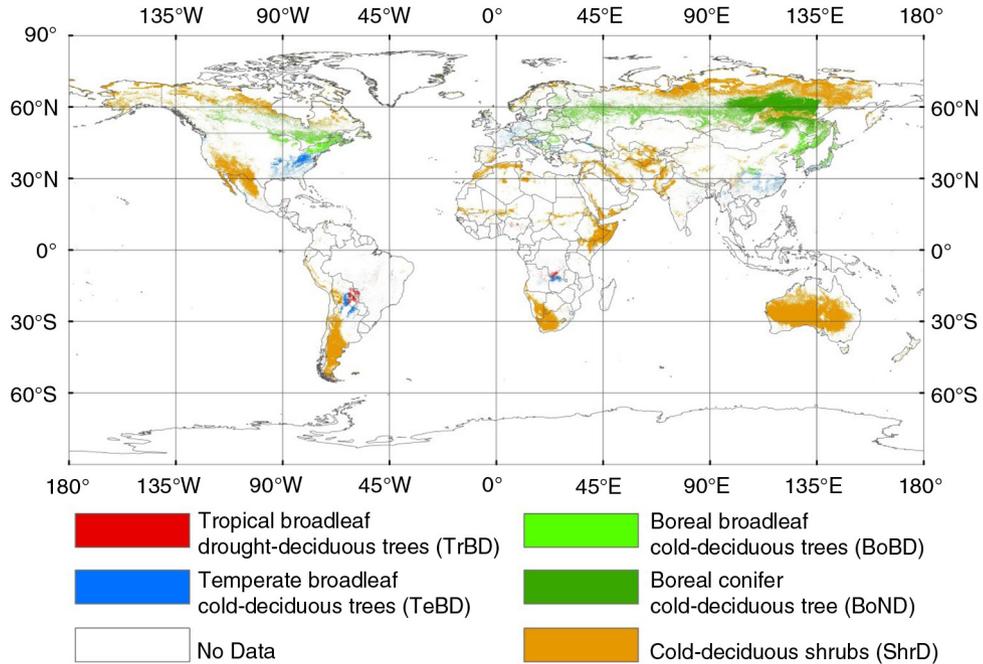

🟥	Tropical broadleaf drought-deciduous trees (TrBD)		🟩	Boreal broadleaf cold-deciduous trees (BoBD)
🟦	Temperate broadleaf cold-deciduous trees (TeBD)		🟩	Boreal conifer cold-deciduous tree (BoND)
⬜	No Data		🟧	Cold-deciduous shrubs (ShrD)

Fig. 1. Plant functional types map of deciduous trees and shrubs derived from MODIS land cover data. Areas in white represent open water and other areas outside the study area.

Table 1. Carbon allocation coefficients and specific leaf area parameters used in IBIS

Plant function type	Allocation to leaf (aleaf)	Allocation to stem (astem)	Allocation to root (aroot)	Specific leaf area (SLA, m^2 kg C^{-1})
Tropical broadleaf drought-deciduous trees	0.30	0.50	0.20	25
Temperate broadleaf cold-deciduous trees	0.30	0.50	0.20	25
Boreal broadleaf cold-deciduous trees	0.30	0.50	0.20	25
Boreal conifer cold-deciduous tree	0.30	0.50	0.20	25
Cold-deciduous shrubs	0.45	0.20	0.35	25

changes (Pinzon et al., 2005; Tucker et al., 2005). We selected the maximum value of two 16-d periods from each month as the monthly NDVI value for each pixel to minimise the atmospheric and cloud contamination effects (Holben, 1986). The AVHRR GIMMS LAI products, with 16-km resolution from 2000 to 2006, are based on a monthly maximum value composed of AVHRR spectral reflectance data to mitigate cloud cover, smoke and other atmospheric aerosol contamination effects (www.cybele.bu.edu; Myneni et al., 1997).

We used input datasets of total cloud fraction (*cld*), net radiation (R_n), wind speed (W_s), vapor pressure deficit (*VPD*), pressure (*P*), air temperature (T_a), relative humidity (R_h), precipitation (*PPT*) and photosynthetically active radiation (*PAR*) from the MERRA (Modern Era Retrospective-Analysis for Research and Applications) archive for 2000–2006 (Global Modeling and Assimilation Office, 2004). MERRA is a NASA reanalysis for the satellite era using a new version of the Goddard Earth Observing System Data Assimilation System Version 5 (GEOS-5) at a resolution of 0.5° latitude by 0.67° longitude. The gridded AVHRR GIMMS NDVI data were resampled to the spatial resolution of MERRA.

This study inversely predicted the carbon allocation parameters over five deciduous vegetation types, including tropical broadleaf drought-deciduous trees (TrBD), temperate broadleaf cold-deciduous trees (TeBD), boreal broadleaf cold-deciduous trees (BoBD), boreal conifer cold-deciduous trees (BoND) and cold-deciduous shrubs (ShrD) (Fig. 1). We combined the MODIS land cover product (MOD11) with the Köppen-Geiger climate classification scheme to derive a global plant functional type (PFT) distribution map (Liu et al., 2014). The global PFT categories map with 1-km resolution was resampled to MERRA's resolution, and the PFT of the MERRA grid were determined using the type of PFT in the PFT categories map that had the greatest area in each MERRA grid.

We compiled an extensive database of biomass values for validating the performance of the modified version of IBIS model (Fig. 2). The biomass observations of deciduous forests are collected by Luo (1996) in China and Usoltsev (2010) in Eurasia. The biomass data of deciduous shrubs covers Australia (Barrett et al., 2001), New Zealand

(Watt et al., 2003), China (Shang-guan and Zhang, 1989; Luo et al., 2002, 2005), the United States of America (Bradley et al., 2006) and Spain (Cerrillo and Oyonarte, 2006).

2.4. Parameter inversion method

The MCMC method is used to inversely predict the carbon allocation model parameters for non-limiting conditions using satellite-based LAI. The posterior probability density functions (PDFs) for model parameters were generated from prior PDFs with LAI observations using a MCMC sampling technique. This study used the Metropolis-Hastings (MH) algorithm (Metropolis et al., 1953; Hastings, 1970) as the MCMC sampler. We first specified ranges for carbon allocation model parameters using prior knowledge. The initial, lower and upper values were 0.3, 0.1 and 0.49 for both r_0 and s_0, respectively. We then used the MCMC method to generate high-dimensional PDFs of model parameters via a sampling procedure (Xu et al., 2006; Yuan et al., 2012a). After we ran the model 100,000 times, the model parameters estimated by the MH algorithm converged to stationary distributions (Yuan et al., 2012b). We randomly selected half of the grid cells of each PFT for the inversion of RACA model parameters and used the other half of the grid cells for the validation of the RACA model parameters.

3. Results

3.1. Carbon allocation parameters and model performance

For all five vegetation types, carbon allocation coefficients of leaves (l_0), stems (s_0) and roots (r_0) under the non-limiting environmental condition were well constrained within the prior parameter ranges (Fig. 3). All three inversely predicted parameters indicated significant differences among different PFTs (Table 2). The largest l_0 was found for TrBD, with a mean value of 0.420 ± 0.004 (mean value $\pm$ standard deviation), and the lowest for ShrD, with a mean value of 0.296 ± 0.018. In contrast, TrBD and ShrD showed
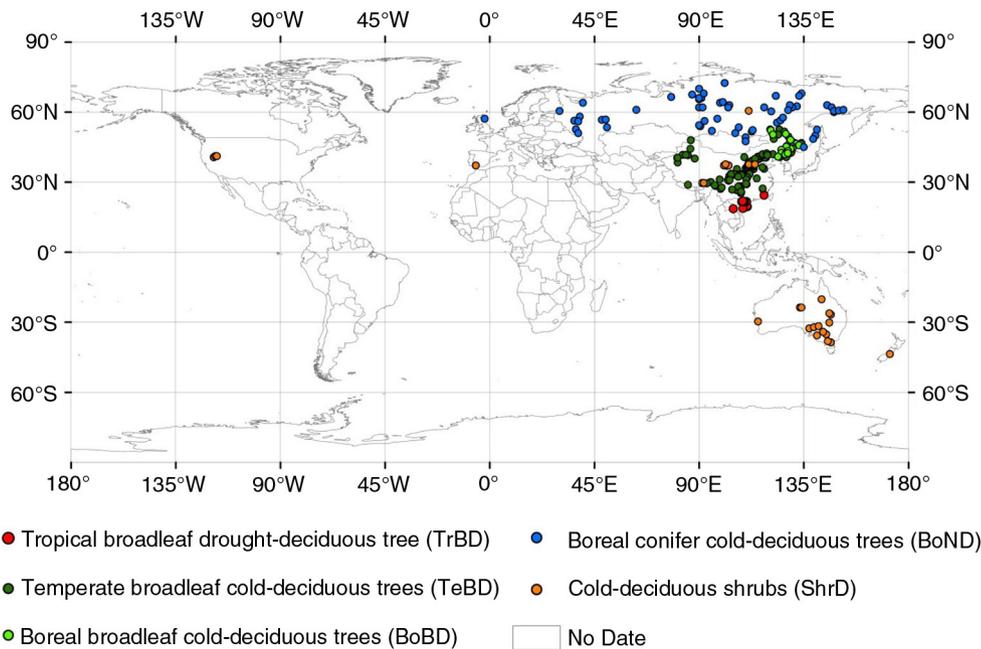
Fig. 2. The locations of biomass sampling plots collected in this study.

the lowest and the highest r_0, with mean values of 0.167 ± 0.008 and 0.317 ± 0.004, respectively.

The RACA model substantially improved the accuracy of LAI simulations of all five vegetation types (Fig. 4). The LAI simulated using the RACA model (LAI_{RACA}) showed significantly lower root-mean-square error (RMSE) and higher R^2 than those using the original IBIS carbon allocation coefficients (i.e. LAI_{IBIS}). Compared with the LAI_{IBIS}, the RMSEs of LAI_{RACA} were reduced – 64, 67, 61, 62 and 68% for TrBD, TeBD, BoBD, BoND and ShrD, respectively (Fig. 4a), and the R^2 of LAI_{RACA} were increased – 215, 169, 74, 42 and 144% for TrBD, TeBD, BoBD, BoND and ShrD, respectively (Fig. 4b).

The maximum LAI simulated using the resource availability carbon allocation model (LAI_{RACA}) showed comparable magnitude with satellite-based maximum LAI (LAI_{RS}). The spatial distribution of the differences between the simulated maximum LAI and LAI_{RS} showed that LAI_{RACA} performed much better than the maximum LAI simulated by the original IBIS (LAI_{IBIS}) (Fig. 5a and c). LAI_{RACA} increased the percentage of errors around zero and decreased large positive and negative errors (Fig. 5b and d). For example, 82.2% of the difference values between LAI_{RACA} and LAI_{RS} were distributed in the range of -0.5 to 0.5, which was much larger than the value (19.5%) between LAI_{IBIS} and LAI_{RS}.

Moreover, we investigated if the revised carbon allocation model can improve the accuracy of biomass simulations. Over the 650 sites globally, the results show that the IBIS model with the resource availability carbon allocation model ($IBIS_{RACA}$) significantly improved the performance of simulating aboveground biomass of all five vegetation types, except for TrBD (Fig. 6). Compared with the biomass simulated by the original IBIS model, the RMSE values of biomass estimates simulated by the $IBIS_{RACA}$ model were decreased by 62, 73.6, 35 and 20% for TeBD, BoBD, BoND and ShrD, respectively.

3.2. Spatial patterns of resource availabilities and carbon allocation coefficients

Both light and water availabilities showed high spatial heterogeneity (Fig. 7). For the annual mean (ANN) resource availabilities, there was light limitation in the high-latitude northern hemisphere, equator and southern South America, and water limitation south of 45° N (Fig. 7a and b). The majority of the study area suffered from nitrogen limitation (Fig. 7c). The resource availabilities showed seasonal variations. The highest light, water and nitrogen availabilities occurred in June–August (JJA) over the high-latitude areas (Fig. 7g–i), whereas the lowest water availabilities occurred in March–May (MAM) (Fig. 7e). The light and nitrogen availabilities in September–November (SON) (Fig. 7j and l) were consistent with those in MAM (Fig. 7d and f). The highest nitrogen availabilities and lowest light availabilities were found in DJF in the southern hemisphere (Fig. 7m and o). The water availabilities in DJF and SON (Fig. 7k and n) were lower than those in MAM and JJA (Fig. 7e and h).
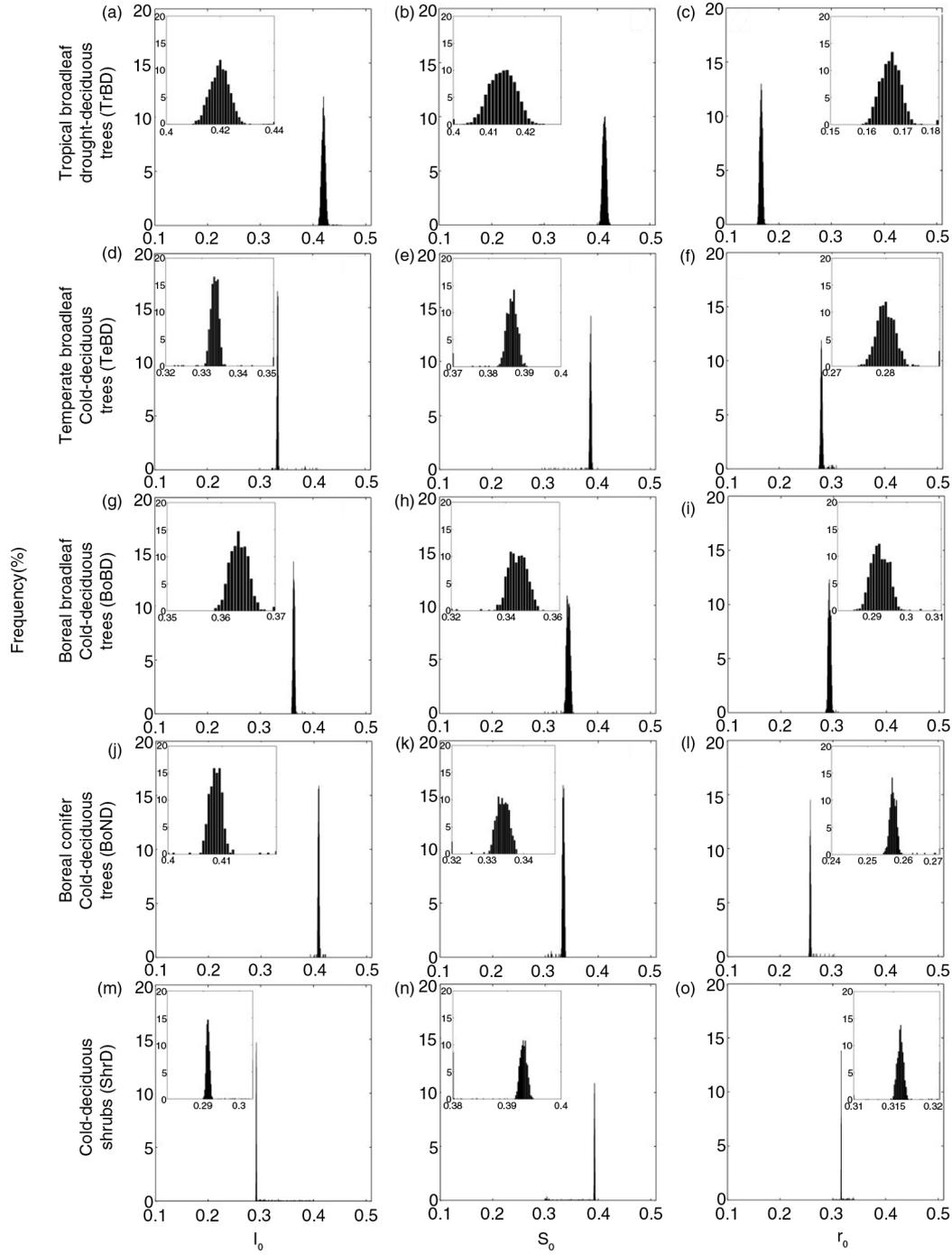
Fig. 3. Histogram to indicate frequency distribution of parameters derived from Bayesian Markov chain Monte Carlo inversion. l_0, s_0 and r_0 are carbon allocation coefficients to leaf, stem and root for non-limiting condition. The insets show the frequency distributions of parameters with smaller X-axis range.

The spatial and seasonal patterns of carbon allocation ratios depended on the vegetation types (Fig. 8). The highest allocation to stems and the lowest allocation to roots occurred in the summer (i.e. JJA) in the high-latitude northern hemisphere (Fig. 8h and i), whereas the highest root allocation and lowest stem allocation occurred in MAM (Fig. 8e and f). For ShrD in the southern hemisphere, the highest leaf allocation and stem allocation, and the lowest root allocation occurred in the summer (i.e. DJF) (Fig. 8m–o). For annual mean carbon allocation ratios, the root allocation

Table 2. Comparison of the inversely predicted carbon allocation coefficients under the optimal environments

Plant function type	Leaf (l_0)*	Stem (s_0)	Root (r_0)
Tropical broadleaf drought-deciduous trees	0.420 ± 0.004[a]	0.413 ± 0.009[a]	0.167 ± 0.008[a]
Temperate broadleaf cold-deciduous trees	0.334 ± 0.007[b]	0.385 ± 0.009[b]	0.281 ± 0.004[b]
Boreal broadleaf cold-deciduous trees	0.363 ± 0.003[c]	0.344 ± 0.004[c]	0.292 ± 0.003[c]
Boreal conifer cold-deciduous tree	0.409 ± 0.002[d]	0.334 ± 0.004[d]	0.258 ± 0.004[d]
Cold-deciduous shrubs	0.296 ± 0.018[e]	0.387 ± 0.020[e]	0.317 ± 0.004[e]

The letters indicate statistical significance of inversely predicted parameters among vegetation types ($p < 0.05$). *The mean value with standard deviation among all grid cells of each plant function type.

was larger than the leaf and stem allocation in ShrD and TrBD (Fig. 8a–c). More carbon was allocated to leaves and stems in TeBD and BoBD in eastern Asia. BoND allocated more carbon to roots and leaves than to stems.

3.3. Carbon allocation coefficient variation with resource availabilities

Figure 9 shows the theoretical changes in the carbon allocation fraction of three plant components with environment

Fig. 4. Root-mean-square error (RMSE) (a) and coefficient of determination (R^2) (b) of LAI simulations based on two allocation methods. The LAI_{RACA} refers to the LAI simulated by the resource availability carbon allocation model. The LAI_{IBIS} refers to the LAI simulated by the original IBIS carbon allocation coefficients. The letters above the bars indicate the significance of the differences between the LAI estimates ($p < 0.05$).

variables. The root allocation fraction decreased with the reduction of light availability (Fig. 9c, f, i, l, and o), and similarly, stem allocation decreased with the reduction of belowground resource (i.e. water and nutrient) availabilities (Fig. 9b, e, h, k, and n). When both belowground resources and light are abundant, there is maximum allocation to leaves (Fig. 9a, d, g, j, and m). Over the various vegetation types, carbon allocation coefficients show similar changing patterns with resource availabilities; however, the inversely predicted carbon allocation coefficients for non-limiting conditions (i.e. r_0, s_0 and l_0) determined their magnitude.
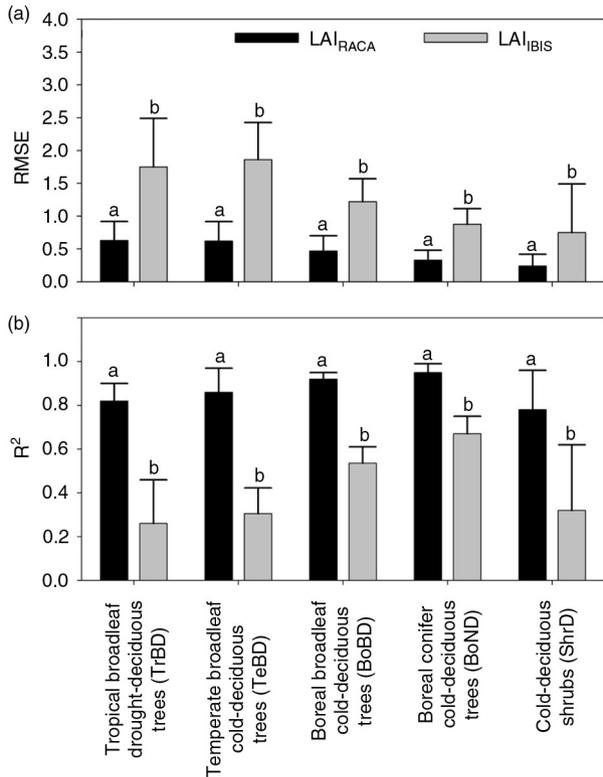
4. Discussion

Our results showed that carbon allocation parameters can be successfully constrained by satellite-based LAI. The inversely predicted parameters are different than those used in previous studies. For example, the CASA-RACA (Friedlingstein et al., 1999) and ORCHIDEE model (Krinner et al., 2005) defined the same carbon allocation parameters (i.e. r_0, s_0 and l_0) for all vegetation types. Moreover, several ecosystem models used consistent carbon allocation methods (Fig. 10), and the allocation coefficients showed substantial differences with the inversely predicted parameters in this study. Most of the ecosystem models allocated the largest fractions of carbon to the stems for all four deciduous vegetation types (Fig. 10a–d). However, our results showed the lowest allocation coefficients for stems (Fig. 10f–i). In shrublands, this study estimated the carbon allocation coefficients of stems, leaves and roots to be equal to 0.192 ± 0.099, 0.222 ± 0.059 and 0.586 ± 0.153, respectively (Fig. 10j and Table 3). The carbon allocation coefficients in other models showed large differences among the three plant components (Fig. 10e).

Our study demonstrated that the RACA model significantly improved the accuracy of LAI and biomass estimates. The aboveground biomass in the original IBIS model was overestimated. In forests, carbon allocated to stems mainly contributed to the carbon sequestration because the woody tissues have a long turnover time (Schulze et al., 2000). The $IBIS_{RACA}$ model allocated a lower fraction of carbon to
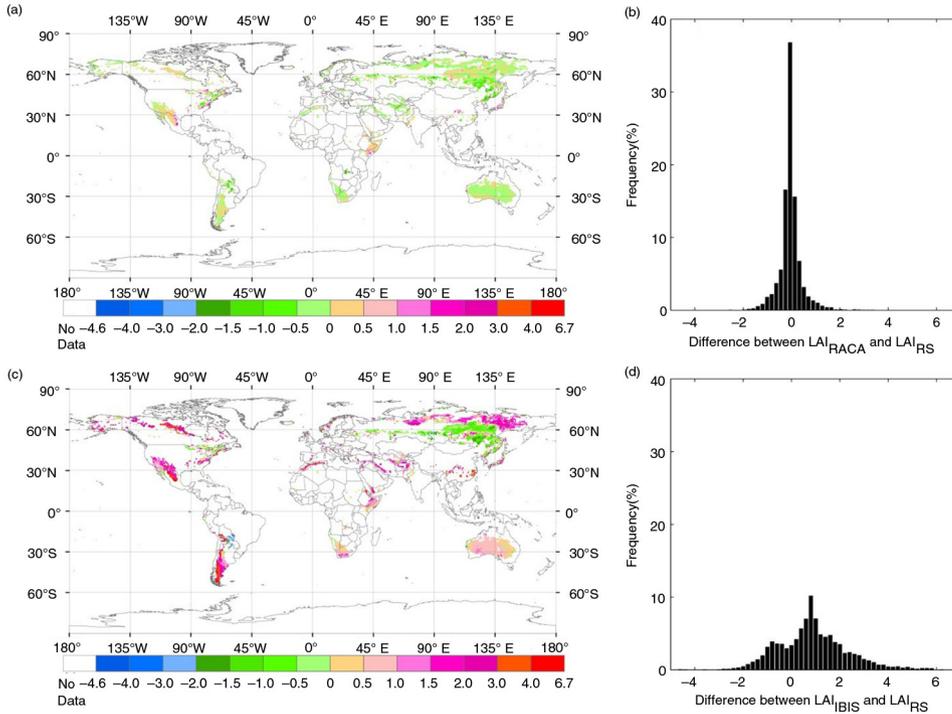
Fig. 5. Difference between the simulated maximum leaf area index (LAI) and satellite-based maximum LAI (LAI$_{RS}$). (a) and (b) are the spatial and frequency distributions of difference between the maximum LAI simulated using the resource availability carbon allocation model (LAI$_{RACA}$) and LAI$_{RS}$, respectively. (c) and (d) are the spatial and frequency distributions of difference between the maximum LAI simulated by the original IBIS (LAI$_{IBIS}$) and LAI$_{RS}$, respectively.
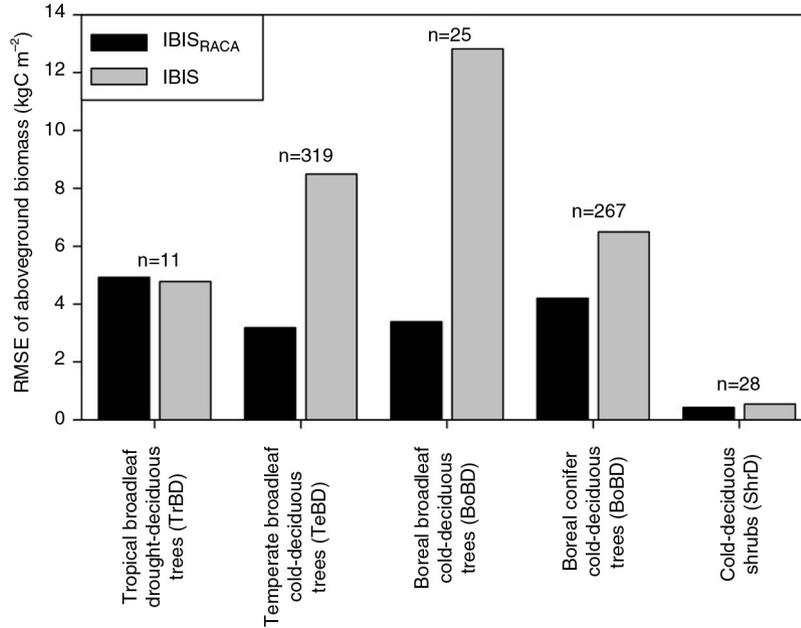

Fig. 6. Root-mean-square error (RMSE) of aboveground biomass simulations by the IBIS model. IBIS$_{RACA}$ denotes IBIS model with resource availability carbon allocation model. The IBIS denotes the original IBIS model with constant carbon allocation coefficients. The 'n' above the bars is the site number for model validation.
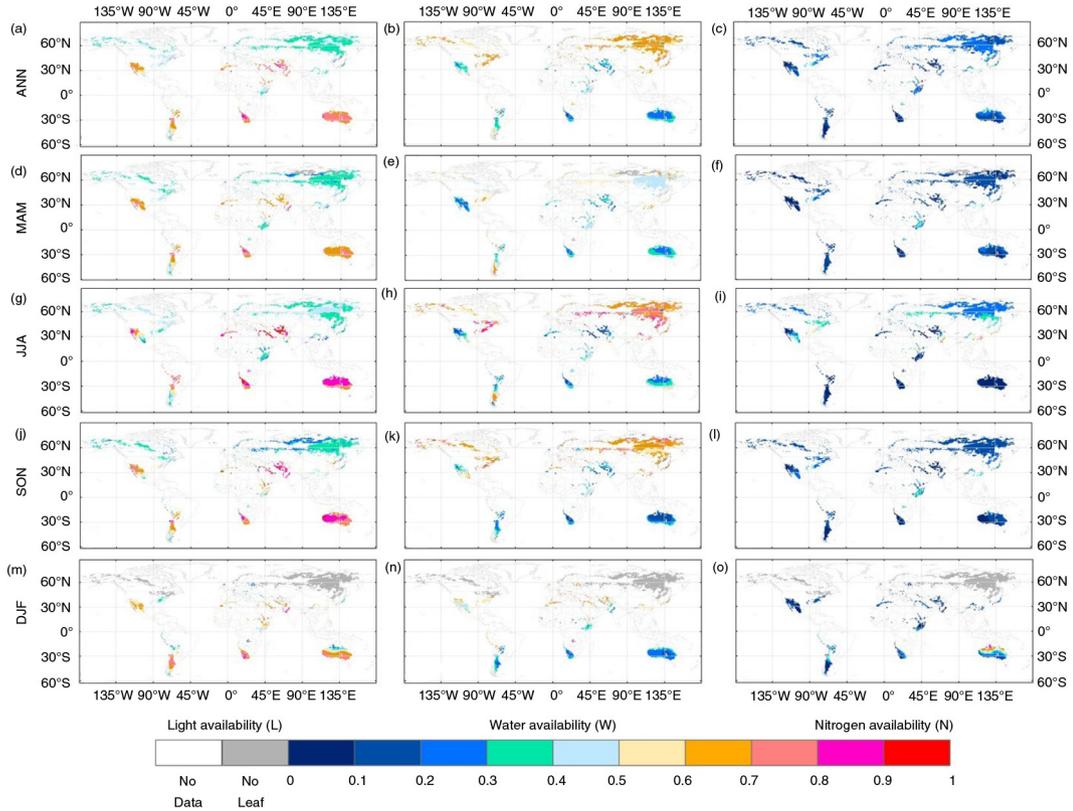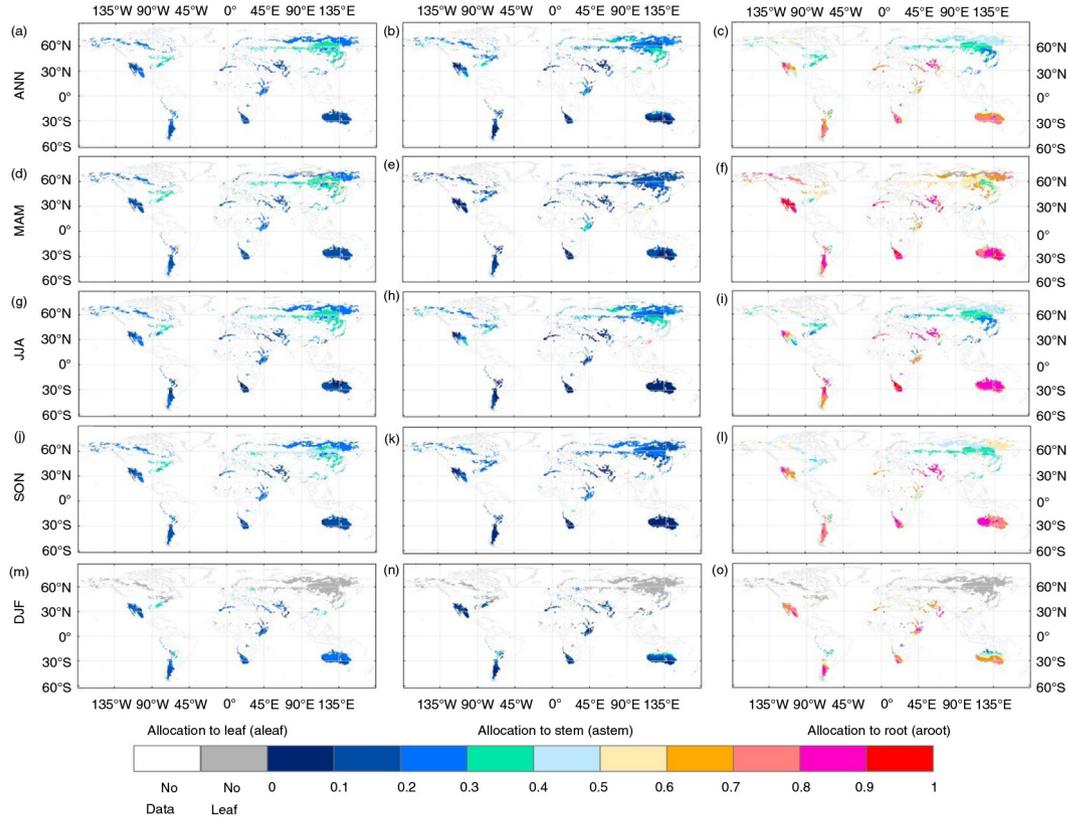
Fig. 7. Spatial distribution of the annual mean (ANN) light (L), water (W) and nitrogen (N) availabilities from 2000 to 2006 (a–c) and in March–May (MAM) (d–f), June–August (JJA) (g–i), September–November (SON) (j–l) and December–February (DJF) (m–o).

stems than that in the original IBIS model (Tables 1 and 3). This is how the RACA model improved the performance of the IBIS model in simulating biomass.

The RACA model did not consider the observed allometric relationships among plant components, such as the power-law relationship between leaf biomass and the remaining (i.e. stem and root) biomass (Reichle, 1981; Janecek et al., 1989) and the pipe model (Shinozaki et al., 1964a, 1964b; Morataya et al., 1999). However, no gross inconsistencies among the biomass of plant components appear in the IBIS$_{RACA}$ model. The exponent values of power-law equations between leaves and the remaining biomass from the IBIS$_{RACA}$ model (i.e. 1.41 for TeBD and 1.60 for BoBD; data not shown) were very close to the observed exponent values (i.e. 1.60 for all of the woody PFTs) in the FBM model (Janecek et al., 1989; Lüdeke et al., 1994). Sapwood biomass was a fraction of stem biomass. The sapwood fraction values in the IBIS model (mean value is 0.06) were close to those in the IBIS$_{RACA}$ model (mean value is 0.07). Thus, the relationships between leaf and sapwood biomass (or the pipe model) were similar to the relationships between leaves and the remaining biomass (data not shown).

There are a number of observed large-scale patterns in nitrogen availability and carbon allocation that are qualitatively comparable with our results. For example, the spatial patterns of allocation coefficients among plant parts show that the root allocation in shrublands is higher than that in forests, which is supported by Gower et al. (1999) and Zhou and Luo (2008). Our nitrogen-limited regions are consistent with the study of Wang et al. (2010). However, it should be noted that the method used to indicate nitrogen availability is empirical and indirect and does not integrate some major nitrogen cycle processes, such as the effect of plant litter input, stoichiometry on soil N mineralization and nitrogen deposition. Therefore, future studies should incorporate the process-based nitrogen cycle model into the allocation model.

This study only inversely predicted the carbon allocation parameters over five deciduous vegetation types because the deciduous plants have explicit seasonality of LAI, and satellite-based LAI data can be used to inversely predict the model parameters. For global-scale application, it is imperative to constrain carbon allocation patterns for other vegetation types. A recent study, for example, used satellite-based fraction of absorbed photosynthetically

Fig. 8.   Spatial distribution of the annual mean (ANN) carbon allocation ratios to leaf (aleaf), stem (astem) and root (aroot) from 2000 to 2006 (a–c) and in March–May (MAM) (d–f), June–August (JJA) (g–i), September–November (SON) (j–l) and December–February (DJF) (m–o).

active radiation (fPAR) and eddy-covariance-based esti-mates of carbon and water fluxes to constrain allocation to roots versus shoots for savannah trees and grasses (Haverd et al., 2015). Our study highlights the fact that increasing field and experiment measurements, which are highly related to carbon allocation, can be used to estimate allocation parameters.

It is important to exclude the model errors of environmental variables for improving the carbon allocation model. So we used the satellite-based ET model to calculate ET and the ratio of ET and PET to indicate water availability. Water availability is one of the most important variables, which regulates the carbon allocation of plants (Poorter et al., 2012). IBIS can simulate ET and plant water availability, however, compared with the IBIS, the satellite-based ET model (i.e. Revised RS-PM) performs better in simulating ET because remotely sensed data provide us with temporally and spatially continuous information over vegetated surfaces (Yuan et al., 2010). So the satellite-based ET model can exclude the model errors of water avail-ability. Moreover, many studies have showed that the ratio of ET and PET, which is used in the carbon allocation

model, can reflect the water condition of the terrestrial ecosystems (Jackson et al., 1981; Anderson et al., 2007; Mu et al., 2013). However, the further model improvements will use simulated water availability by IBIS. Therefore, it is quite interesting and necessary to compare the difference of water availability between these two methods. In addi-tion, light availability is another important regulation of the carbon allocation process. It is governed by at least three important variables, including cloud cover, sun angle and day length. Sun angle is related to the latitudes and day length depends on time (day of year), and both of them have been integrated into the models when calculating daily potential solar radiation. The only variable randomly varied with weather is cloud cover; therefore, the light availability in this study only considered the cloud cover.

5.   Summary and conclusions

In this study, we implemented a revised resource availability carbon allocation model into the IBIS model for five deci-duous vegetation types. The new carbon allocation model was integrated with LAI simulations, allowing for inverting
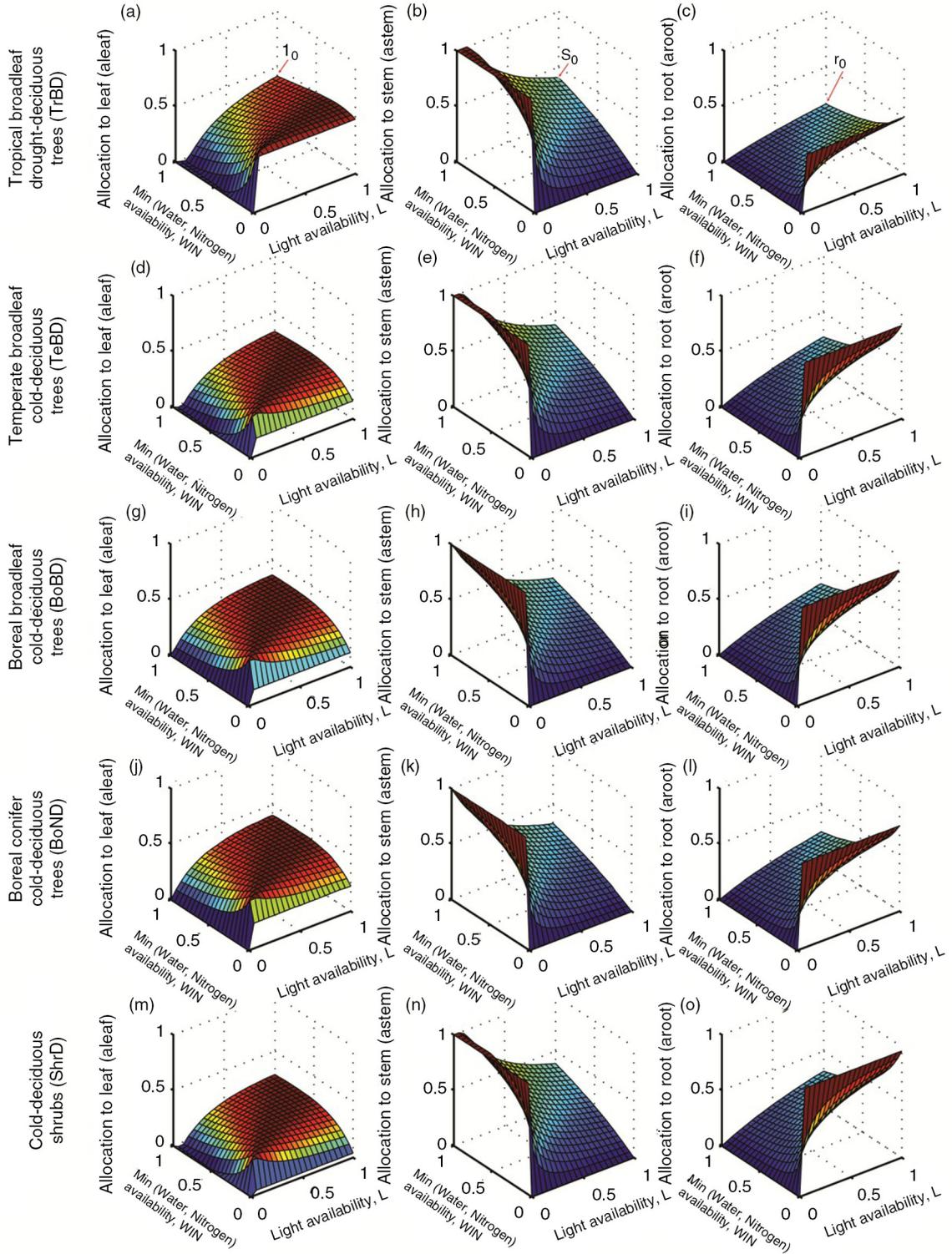
Fig. 9. Allocation fractions for leaf, stem and root components as functions of light (L) and minimum value of water and nitrogen (WN) availabilities for five deciduous plant functional types.

of the allocation parameters using a remotely sensed LAI dataset. The results showed that the carbon allocation coefficients of leaves (l_0), stems (s_0) and roots (r_0) under the optimal environmental conditions can be reliably constrained by the remotely sensed LAI. The inversely predicted parameters substantially improved model accuracy of the
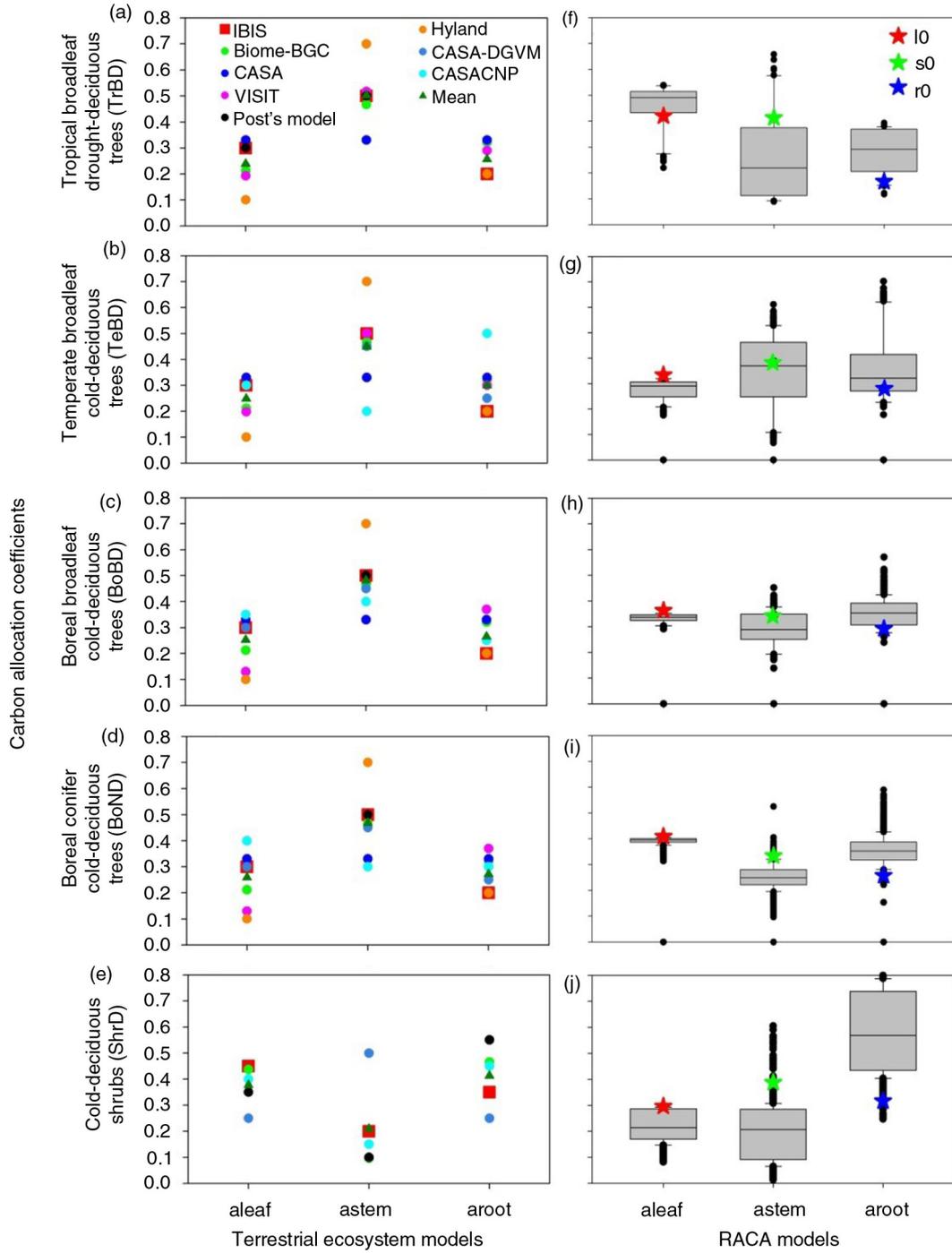
Fig. 10. Carbon allocation ratios (a–e) in a number of terrestrial ecosystem models (CASA (Potter et al., 1993); IBIS (Foley et al., 1996; Kucharik et al., 2000); Hybrid (Friend et al., 1997); Post's model (Post et al., 1997); CASA-DGVM (Potter and Klooster, 1999); Biome-BGC (White et al., 2000); Hyland (Levy et al., 2004); CASACNP (Wang et al., 2010); VISIT (Ise et al., 2010). Carbon allocation ratios of resource availability carbon allocation (RACA) model (f–j) were compared with the terrestrial ecosystem models. r_0, s_0 and l_0 are the carbon allocation ratios for plant grown under non-limiting conditions.

LAI and aboveground biomass simulations globally. The RMSE of LAI simulated by the new allocation model was significantly decreased by approximately 61–68%.

The RMSE of aboveground biomass simulated by the new allocation model was significantly decreased by approximately 20–73.6%. The spatial pattern of allocation

Table 3. Comparison of the annual mean resource availability carbon allocation coefficients under the limiting condition

Plant function type	Allocation to leaf (aleaf)	Allocation to stem (astem)	Allocation to root (aroot)
Tropical broadleaf drought-deciduous trees (TrBD)	0.453 ± 0.094[a]	0.269 ± 0.170[a]	0.278 ± 0.084[a]
Temperate broadleaf cold-deciduous trees (TeBD)	0.282 ± 0.061[b]	0.356 ± 0.147[c]	0.362 ± 0.139[b]
Boreal broadleaf cold-deciduous trees (BoBD)	0.338 ± 0.091[c]	0.300 ± 0.098[b]	0.362 ± 0.111[b]
Boreal conifer cold-deciduous tree (BoND)	0.392 ± 0.033[d]	0.253 ± 0.051[a]	0.355 ± 0.062[b]
Cold-deciduous shrubs (ShrD)	0.222 ± 0.059[e]	0.192 ± 0.099[d]	0.586 ± 0.153[c]

Different letters indicate significant difference between the mean values ($p < 0.05$).

coefficients among plant parts and nitrogen availability is qualitatively comparable with a number of studies. Compared with the standard version of IBIS using fixed allocation ratios, the new allocation model tends to promote higher root carbon allocation. This study presents a method for inverting parameters of the carbon allocation model for five deciduous vegetation types. For global-scale application, it is imperative to constrain carbon allocation patterns for other vegetation types in the future.

6. Acknowledgements

References

Anderson, M. C., Norman, J. M., Mecikalski, J. R., Otkin, J. A. and Kustas, W. P. 2007. A climatological study of evapotranspiration and moisture stress across the continental United States based on thermal remote sensing: 1. Model formulation. *J. Geophys. Res.* **112**, D10117.

Arora, V. K. and Boer, G. J. 2005. A parameterization of leaf phenology for the terrestrial ecosystem component of climate models. *Global Change Biol.* **11**, 39–59.

Barrett, D. J., Galbally, I. E. and Graetz, R. D. 2001. Quantifying uncertainty in estimates of C emissions from above-ground biomass due to historic land-use change to cropping in Austraila. *Global Change Biol.* **7**, 883–902.

Bazzaz, F. A. and Grace, J. 1997. *Plant Resource Allocation*. Academic Press, San Diego, CA.

Bonan, G. B. 2008. *Ecological Climatology: Concepts and Applications*. Cambridge University Press, Cambridge, pp. 278–281.

Bradley, B. A., Houghton, R. A., Mustard, J. F. and Hamburg, S. P. 2006. Invasive grass reduces aboveground carbon stocks in shrublands of the Western US. *Global Change Biol.* **12**(10), 1815–1822.

Cannell, M. G. R. and Dewar, R. 1994. Carbon allocation in trees: a review of concepts for modelling. *Adv. Ecol. Res.* **25**, 59–104.

Cerrillo, R. M. N. and Oyonarte, P. B. 2006. Estimation of above-ground biomass in shrubland ecosystems of southern Spain. *Forest Syst.* **15**(2), 197–207.

Chapin, F. S. 1991. Integrated responses of plants to stress. *BioScience.* **41**(1), 29–36.

Chen, Y., Xia, J., Liang, S., Feng, J., Fisher, J. B. and co-authors. 2014. Comparison of satellite-based evapotranspiration models over terrestrial ecosystems in China. *Remote Sens. Environ.* **140**, 279–293.

De Kauwe, M. G., Medlyn, B. E., Zaehle, S., Walker, A. P., Dietze, M. C. and co-authors. 2014. Where does the carbon go? A model–data intercomparison of vegetation carbon allocation and turnover processes at two temperate forest free air CO_2 enrichment sites. *New Phytol.* **203**, 883–899.

Doughty, C. E., Metcalfe, D. B., da Costa, M. C., de Oliveira, A. A. R., Neto, G. F. C. and co-authors. 2013. The production, allocation and cycling of carbon in a forest on fertile terra preta soil in eastern Amazonia compared with a forest on adjacent infertile soil. *Plant Ecol. Divers.* **7**(1–2), 41–53.

Foley, J. A., Prentice, I. C., Ramankutty, N., Levis, S., Pollard, D. and co-authors. 1996. An integrated biosphere model of land surface processes, terrestrial carbon balance, and vegetation dynamics. *Global Biogeochem. Cycles.* **10**, 603–628.

Franklin, O., Johansson, J., Dewar, R. C., Dieckmann, U., McMurtrie, R. E. and co-authors. 2012. Modeling carbon allocation in trees: a search for principles. *Tree Physiol.* **32**(6), 648–666.

Friedlingstein, P., Joel, G., Field, C. and Fung, I. 1999. Toward an allocation scheme for global terrestrial carbon models. *Global Change Biol.* **5**, 755–770.

Friend, A., Stevens, A., Knox, R. and Cannell, M. 1997. A process-based, terrestrial biosphere model of ecosystem dynamics (Hybrid v3. 0). *Ecol. Model.* **95**, 249–287.

Fung, I. Y., Doney, S. C., Lindsay, K. and John, J. 2005. Evolution of carbon sinks in a changing climate. *Proc. Natl. Acad. Sci. USA.* **102**, 11201–11206.

Global Modeling and Assimilation Office. 2004. *File Specification for GEOSDAS Gridded Output Version 5.3, Report*. NASA Goddard Space Flight Cent, Greenbelt, MD.

Gorissen, A., Tietema, A., Joosten, N. N., Estiarte, M., Penuelas, J. and co-authors. 2004. Climate change affects carbon allocation to the soil in shrublands. *Ecosystems.* **7**, 650–661.

Gower, S. T., Kucharik, C. J. and Norman, J. M. 1999. Direct and indirect estimation of leaf area index, f APAR, and net primary production of terrestrial ecosystems. *Remote Sens. Environ.* **70**, 29–51.

Hastings, W. K. 1970. Monte Carlo sampling methods using Markov chains and their applications. *Biometrika.* **57**, 97–109.

Haverd, V., Smith, B., Raupach, M., Briggs, P., Nieradzik, L. and co-authors. 2015. Coupling carbon allocation with leaf and root phenology predicts tree-grass partitioning along a savanna rainfall gradient. *Biogeosci. Discuss.* **12**, 16313–16357.

Haxeltine, A. and Prentice, I. C. 1996. BIOME3: an equilibrium terrestrial biosphere model based on ecophysiological constraints, resource availability, and competition among plant functional types. *Global Biogeochem. Cycles.* **10**, 693–709.

Holben, B. N. 1986. Characteristics of maximum-value composite images from temporal AVHRR data. *Int. J. Remote Sens.* **7**, 1417–1434.

Ise, T., Litton, C. M., Giardina, C. P. and Ito, A. 2010. Comparison of modeling approaches for carbon partitioning: impact on estimates of global net primary production and equilibrium biomass of woody vegetation from MODIS GPP. *J. Geophys. Res.* **115**(G4), G04025.

Jackson, R. D., Idso, S. B., Reginato, R. J. and Pinter, P. J. 1981. Canopy temperature as a crop water stress indicator. *Water Resour. Res.* **17**, 1133–1138.

Janecek, A., Benderoth, G., Lüdeke, M., Kindermann, J. and Kohlmaier, G. 1989. Model of the seasonal and perennial carbon dynamics in deciduous-type forests controlled by climatic variables. *Ecol. Model.* **49**, 101–124.

Kindermann, J., Lüdeke, M., Badeck, F.-W., Otto, R., Klaudius, A. and co-authors. 1993. Structure of a global and seasonal carbon exchange model for the terrestrial biosphere the frankfurt biosphere model (FBM). *Water Air Soil Poll.* **70**, 675–684.

Krinner, G., Viovy, N., de Noblet Ducoudré, N., Ogée, J., Polcher, J. and co-authors. 2005. A dynamic global vegetation model for studies of the coupled atmosphere biosphere system. *Global Biogeochem. Cycles.* **19**, GB1015.

Kucharik, C. J., Foley, J. A., Delire, C., Fisher, V. A., Coe, M. T. and co-authors. 2000. Testing the performance of a dynamic global ecosystem model: water balance, carbon balance, and vegetation structure. *Global Biogeochem. Cycles.* **14**, 795–825.

Levy, P., Cannell, M. and Friend, A. 2004. Modelling the impact of future changes in climate, CO2 concentration and land use on natural ecosystems and the terrestrial carbon sink. *Global Environ. Change.* **14**, 21–30.

Liu, D., Chen, Y., Cai, W., Dong, W., Xiao, J. and co-authors. 2014. The contribution of China's Grain to Green Program to carbon sequestration. *Landscape Ecol.* **29**, 1675–1688.

Lüdeke, M. K., Badeck, F.-W., Otto, R. D., Hager, C., Donges, S. and co-authors. 1994. The Frankfurt Biosphere Model: a global process-oriented model of seasonal and long-term CO2 exchange between terrestrial ecosystems and the atmosphere. I. Model description and illustrative results for cold deciduous and boreal forests. *Clim. Res.* **4**, 143–166.

Luo, T. X. 1996. *The Spatial Pattern and Mathematical Model of Productions of China's Major Forest Types.* Unpublished Doctoral Dissertation. Science Academy of China, Beijing, China.

Luo, T. X., Brown, S., Pan, Y., Shi, P., Ouyang, H. and co-authors. 2005. Root biomass along subtropical to alpine gradients: global implication from Tibetan transect studies. *Forest Ecol. Manag.* **206**(1), 349–363.

Luo, T. X., Li, W. H. and Zhu, H. Z. 2002. Estimated biomass and productivity of natural vegetation on the Tibetan Plateau. *Ecol. Appl.* **12**(4), 980–997.

Malhi, Y., Doughty, C. and Galbraith, D. 2011. The allocation of ecosystem net primary productivity in tropical forests. *Philos. Trans. R. Soc. Lond. B Biol. Sci.* **366**, 3225–3245.

McMurtrie, R. E. and Dewar, R. C. 2013. New insights into carbon allocation by trees from the hypothesis that annual wood production is maximized. *New Phytol.* **199**, 981–990.

Metropolis, N., Rosenbluth, A. W., Rosenbluth, M. N., Teller, A. H. and Teller, E. 1953. Equation of state calculations by fast computing machines. *J. Chem. Phys.* **21**, 1087–1092.

Monsi, M. and Saeki, T. 1953. Uber den Lichtfaktor in den Pflanzengesellschaften und seine Bedeutung fur die Stoffproduktion [The light factor in the plant communities and its importance for the fabric production]. *Jpn. J. Bot.* **14**, 22–52.

Monteith, J. 1965. Evaporation and environment. *Symp. Soc. Exp. Biol.* **19**, 205–234.

Moorcroft, P., Hurtt, G. and Pacala, S. W. 2001. A method for scaling vegetation dynamics: the ecosystem demography model (ED). *Ecol. Monogr.* **71**, 557–586.

Morataya, R., Galloway, G., Berninger, F. and Kanninen, M. 1999. Foliage biomass-sapwood (area and volume) relationships of *Tectona grandis LF* and *Gmelina arborea* Roxb.: silvicultural implications. *Forest Ecol. Manag.* **113**, 231–239.

Mu, Q., Zhao, M., Kimball, J. S., McDowell, N. G. and Running, S. W. 2013. A remotely sensed global terrestrial drought severity index. *Bull. Am. Meteorol. Soc.* **94**, 83–98.

Myneni, R. B., Ramakrishna, R., Nemani, R. and Running, S. W. 1997. Estimation of global leaf area index and absorbed PAR using radiative transfer models. *IEEE Trans. Geosci. Remote Sens.* **35**, 1380–1393.

Parton, B., Ojima, D., Del Grosso, S. and Keough, C. 2001. *CENTURY Tutorial. Supplement to CENTURY User's Manual.* NREC Pub. Natural Resource Ecology Laboratory, Colorado State Univ., Fort Collins, Colorado, USA, pp. 13.

Pinzon, J., Brown, M. E. and Tucker, C. J. 2005. Satellite time series correction of orbital drift artifacts using empirical mode decomposition. In: *Hilbert-Huang Transform: Introduction and Applications* (ed. N. Huang). World Scientific, Toh Tuck Lake, Singapore, pp. 167–186.

Poorter, H., Niklas, K. J., Reich, P. B., Oleksyn, J., Poot, P. and co-authors. 2012. Biomass allocation to leaves, stems and roots: meta-analyses of interspecific variation and environmental control. *New Phytol.* **193**, 30–50.

Post, W. M., King, A. W. and Wullschleger, S. D. 1997. Historical variations in terrestrial biospheric carbon storage. *Global Biogeochem. Cycles.* **11**, 99–109.

Potter, C. S. and Klooster, S. A. 1999. Dynamic global vegetation modelling for prediction of plant functional types and biogenic trace gas fluxes. *Global Ecol. Biogeogr.* **8**, 473–488.

Potter, C. S., Randerson, J. T., Field, C. B., Matson, P. A., Vitousek, P. M. and co-authors. 1993. Terrestrial ecosystem production: a process model based on global satellite and surface data. *Global Biogeochem. Cycles.* **7**, 811–841.

Reichle, D. E. 1981. *Dynamic Properties of Forest Ecosystems.* Cambridge University Press, Cambridge.

Scheiter, S. and Higgins, S. I. 2009. Impacts of climate change on the vegetation of Africa: an adaptive dynamic vegetation modelling approach. *Global Change Biol.* **15**, 2224–2246.

Schulze, E.-D., Wirth, C. and Heimann, M. 2000. Managing forests after Kyoto. *Science.* **289**, 2058–2059.

Shang-guan, T. L. and Zhang, F. 1989. On synecological features and biomass of *Ostryopsis davidiana* bush-wood in Yunding Mountain, Shanxi province (in Chinese). *J. Shanxi Univ.* **12**(3), 347–352.

Sharpe, P. J. and Rykiel, E. J. Jr. 1991. Modelling integrated response of plants to multiple stresses. In: *Response of Plants to Multiple Stresses* (eds. H. A. Mooney, W. E. Winner and E. J. Pell). Academic Press, San Diego, CA, pp. 205–224.

Shinozaki, K., Yoda, K., Hozumi, K. and Kira, T. 1964a. A quantitative analysis of plant form-the pipe model theory: I. Basic analyses. *Jpn. J. Ecol.* **14**, 97–105.

Shinozaki, K., Yoda, K., Hozumi, K. and Kira, T. 1964b. A quantitative analysis of plant form-the pipe model theory: II. Further evidence of the theory and its application in forest ecology. *Jpn. J. Ecol.* **14**, 133–139.

Sitch, S., Smith, B., Prentice, I. C., Arneth, A., Bondeau, A. and co-authors. 2003. Evaluation of ecosystem dynamics, plant geography and terrestrial carbon cycling in the LPJ dynamic global vegetation model. *Global Change Biol.* **9**, 161–185.

Tilman, D. 1988. *Plant Strategies and the Dynamics and Structure of Plant Communities.* Princeton University Press, Princeton, NJ.

Tucker, C. J., Pinzon, J. E., Brown, M. E., Slayback, D. A., Pak, E. W. and co-authors. 2005. An extended AVHRR 8 km NDVI dataset compatible with MODIS and SPOT vegetation NDVI data. *Int. J. Remote Sens.* **26**, 4485–4498.

Usoltsev, V. A. 2010. *Eurasian Forest Biomass and Primary Production Data (in Russian).* Ural Branch of Russian Academy of Sciences, Yekaterinburg, pp. 18–41.

Wang, Y. P., Law, R. and Pak, B. 2010. A global model of carbon, nitrogen and phosphorus cycles for the terrestrial biosphere. *Biogeosciences.* **7**, 2261–2282.

Waring, R. H. and Running, S. W. 2010. *Forest Ecosystems: Analysis at Multiple Scales.* Academic Press, New York.

Watt, M. S., Clinton, P. W., Whitehead, D., Richardson, B., Mason, E. G. and co-authors. 2003. Above-ground biomass accumulation and nitrogen fixation of broom (*Cytisus scoparius* L.) growing with juvenile *Pinus radiata* on a dryland site. *Forest Ecol. Manag.* **184**(1), 93–104.

White, M. A., Thornton, P. E., Running, S. W. and Nemani, R. R. 2000. Parameterization and sensitivity analysis of the BIOME-BGC terrestrial ecosystem model: net primary production controls. *Earth Interact.* **4**, 1–85.

Wilson, J. B. 1988. A review of evidence on the control of shoot: root ratio, in relation to models. *Ann. Bot.* **61**(4), 433–449.

Xu, T., White, L., Hui, D. and Luo, Y. 2006. Probabilistic inversion of a terrestrial ecosystem model: analysis of uncertainty in parameter estimation and model prediction. *Global Biogeochem. Cycles.* **20**(2), B2007.

Yuan, W., Liang, S., Liu, S., Weng, E., Luo, Y. and co-authors. 2012a. Improving model parameter estimation using coupling relationships between vegetation production and ecosystem respiration. *Ecol. Model.* **240**, 29–40.

Yuan, W., Liu, S., Liang, S., Tan, Z., Liu, H. and co-authors. 2012b. Estimations of evapotranspiration and water balance with uncertainty over the Yukon River Basin. *Water Resour. Manag.* **26**, 2147–2157.

Yuan, W., Liu, S., Yu, G., Bonnefond, J.-M., Chen, J. and co-authors. 2010. Global estimates of evapotranspiration and gross primary production based on MODIS and global meteorology data. *Remote Sens. Environ.* **114**, 1416–1431.

Yuan, W., Liu, S., Zhou, G., Zhou, G., Tieszen, L. L. and co-authors. 2007. Deriving a light use efficiency model from eddy covariance flux data for predicting daily gross primary production across biomes. *Agr. Forest Meteorol.* **143**, 189–207.

Zhou, T. and Luo, Y. 2008. Spatial patterns of ecosystem carbon residence time and NPP driven carbon uptake in the conterminous United States. *Global Biogeochem. Cycles.* **22**(3), GB3032.